

High-rate GPS: How High Do We Need to Go?

Robert Smalley, Jr.

Center for Earthquake Research and Information, University of Memphis

ABSTRACT

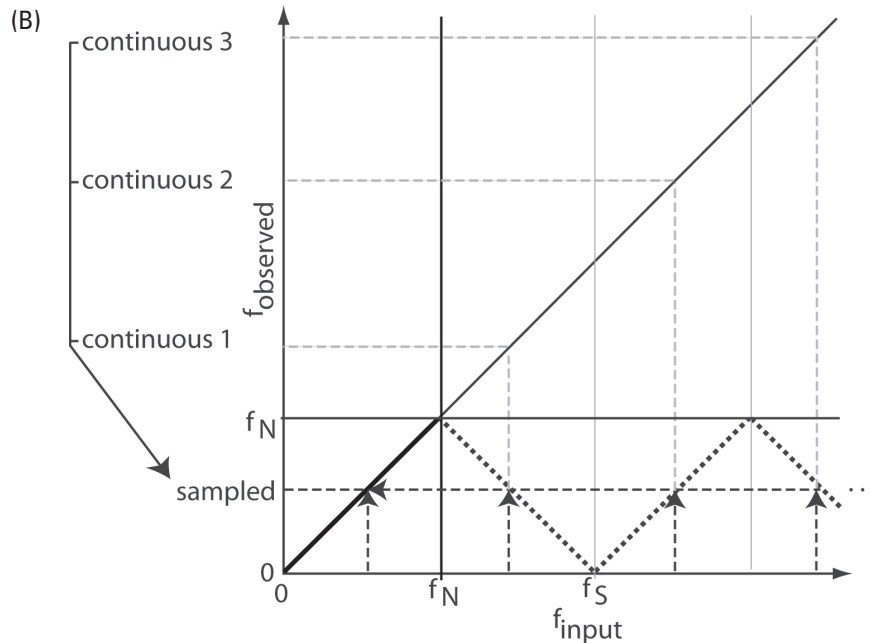
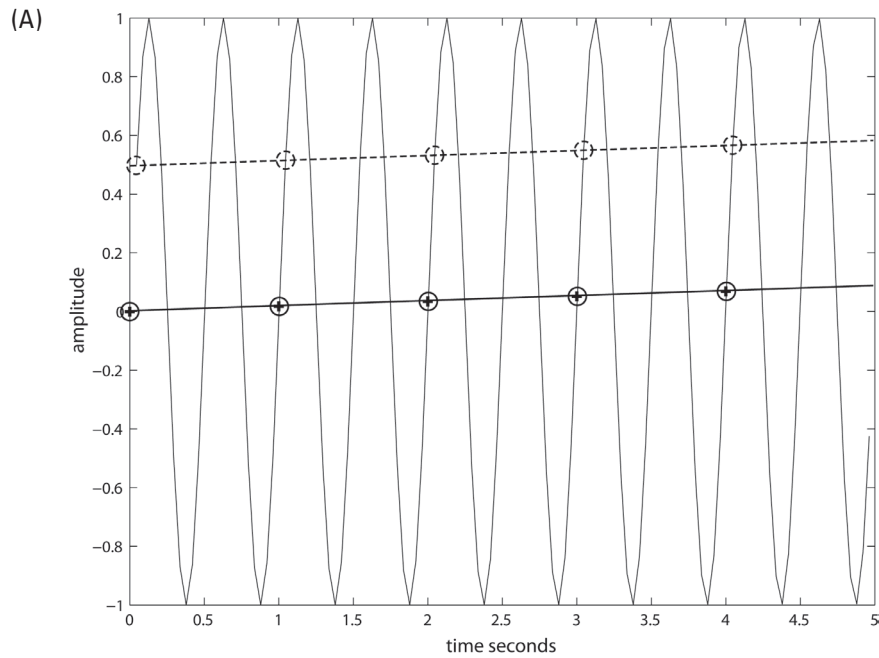
A number of large high-rate GPS (HRGPS) networks, such as the Plate Boundary Observatory (PBO), are poised to capture strong-motion displacements from significant earthquakes with data collected at 1 sec or higher sampling rates. For earthquakes within these networks' footprints, HRGPS data will provide displacement time series at very small epicentral distances that may have great potential to contribute to understanding earthquake rupture processes. The conditional "may" in the previous sentence relates to whether or not the HRGPS data are aliased, *i.e.*, is the sampling fast enough to capture a valid temporal history of displacement? We present analysis of strong-motion recordings in the immediate epicentral area of several large earthquakes to show that 1-Hz sampling would be aliased as suggested. For $M > 7.5$ events, which can be reasonably expected in the PBO footprint, 5-Hz data may also be aliased. These results argue for faster data collection, at least 10 Hz, to record valid displacement time histories at sites that are likely to suffer large co-seismic offsets and large near-field seismic waves. Sampling rates higher than that required by the frequency content of the observable signal provide additional data that can be used to improve the quality of the final HRGPS displacement time series.

INTRODUCTION

Practically all modern data collection is digital, which requires balancing data sampling rates with the frequency domain characteristics of the continuous, analog signal being recorded. Over the past decade, GPS technology and processing have advanced to the stage where it is possible to regularly obtain GPS displacement time series, with precision of a few millimeters, at each epoch for sampling rates of 1 Hz (Bock *et al.* 2004). Precision of better than 1 mm at 1 Hz has been reported by averaging data collected at rates of up to 50 Hz (Genrich and Bock 2006; Bock *et al.* 2006). The majority of the effort, known as GPS seismology, has been applied to increasing the position solution rate and reducing the noise of the displacement time series estimated from the high-rate GPS (HRGPS) phase data. One question that has not been addressed is the sampling rate needed to ensure the resulting HRGPS displacement time series are not aliased at the level of HRGPS resolu-

tion. This is an important question whose answer significantly impacts application of the data. In addition, sampling at a higher rate than necessary to avoid aliasing allows signal processing of the "extra" data to improve the quality of a time series at the lower frequency range of the final time series. Higher sampling rates will also facilitate the use of HRGPS data for applications such as ionospheric studies. We will examine seismic signals, recorded by accelerometers at very small epicentral distances from the fault rupture, and simple models for co-seismic displacement, to guide a discussion of the selection of sampling rates for HRGPS. This discussion will not examine HRGPS data but will discuss the conditions that have to be met to ensure HRGPS produces valid data for spectral analysis. The work reported here complements other work being done to improve GPS processing.

One of the basic theorems of signal processing states that to faithfully represent a continuous analog signal with a uniform sampling of that signal, the signal cannot have energy in its frequency domain representation at frequencies higher than half the sampling frequency. This frequency limit is called the Nyquist frequency, or simply Nyquist (Shannon 1949; Nyquist 1928; Unser 2000). As the restriction on the continuous signal is in the frequency domain, it is generally not possible to determine if a sampling will be valid by looking at it in the time domain. If analog signals have resolvable energy at frequencies higher than Nyquist, the instantaneous amplitudes of these frequencies are correctly recorded in the sampled version of the signal. These higher frequency signals masquerade as another frequency in the time and frequency domains of the sampled data, thus the name "aliasing" for this effect. Aliasing is demonstrated in Figure 1A, which shows two 1-Hz samplings of a sine wave with a frequency slightly higher than 2 Hz. When one "connects the dots," the sampled time series looks like a very low frequency sinusoidal signal. While the sampled time series has the correct instantaneous amplitude at each sample, the wrong frequency will be determined upon frequency analysis, or visually when one plots the samples in the time domain. We examined RINEX files sampled at different frequencies by a single receiver, and the epochs that are common among the different sampling rates all have the same phase value. This indicates they are instantaneous measurements of the phase at those epochs, with no conditioning based on the sample rate. The interval during which the phase

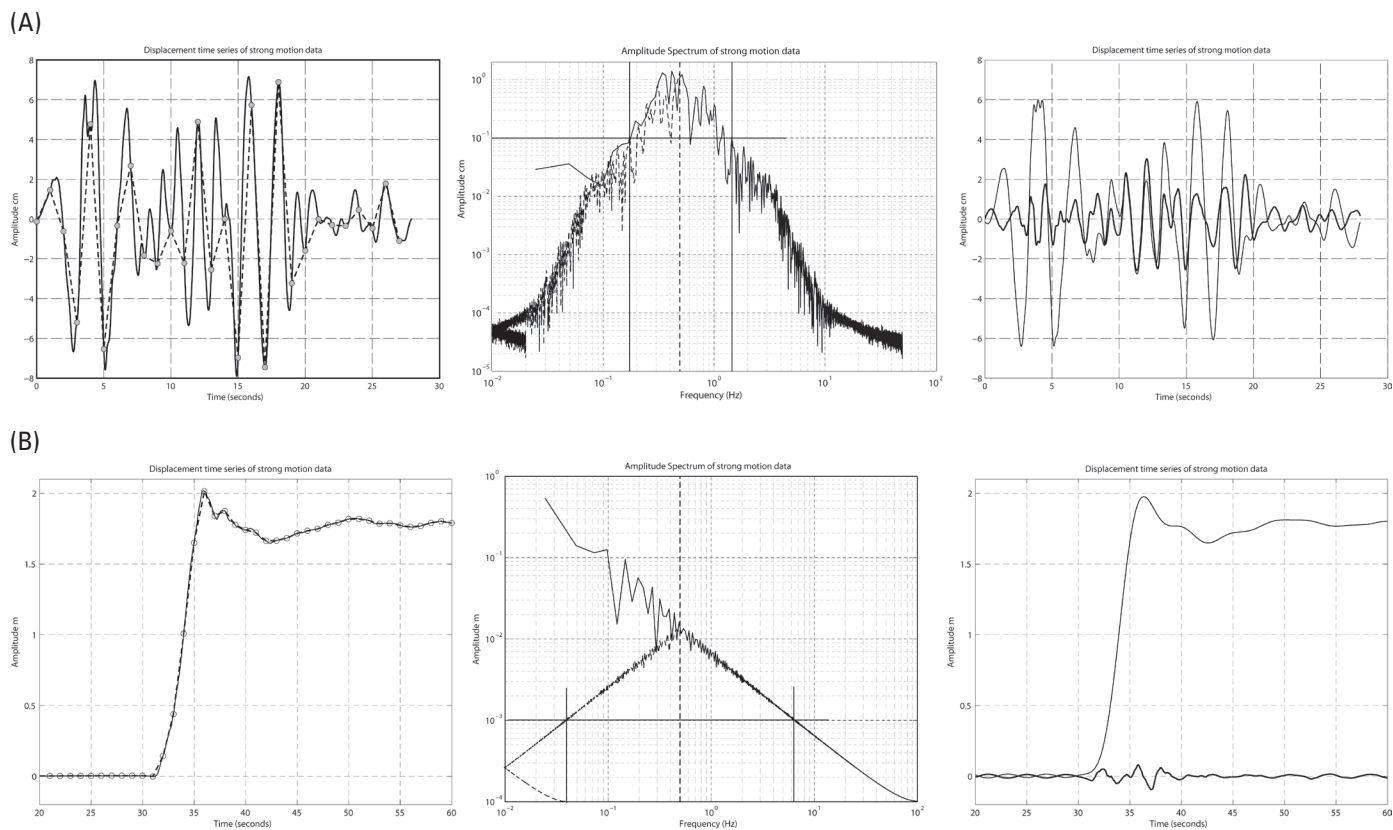


▲ **Figure 1.** A) Illustration of aliasing. A continuous analog sinusoidal signal with a frequency slightly higher than 2 Hz is shown by the thin solid line. Two 1-Hz samplings are shown by the circles on the heavy solid and dashed lines. Since the sampling can be started at any time, there are an infinite number of possible samplings. Analysis of the two aliased recordings will produce the same amplitude and (incorrect) frequency, but different phases. B) Illustration of the mapping between continuous analog input frequency and sampled output frequency. Sampling frequency, f_s , and Nyquist frequency, f_N , are labeled. Observed, aliased output frequency values associated with illegal input frequencies higher than Nyquist are found from the heavy, dashed, sawtooth-shaped line.

measurement is made, the sample-and-hold time, is the same for all sampling rates and much, much smaller than the time between samples.

How aliasing occurs is shown graphically in Figure 1B and the center panels of Figures 2A, 2B, 3A, and 3B. For continuous analog signals with frequencies from 0 to Nyquist, the analog frequency maps into the same value in sampled frequency (ini-

tial heavy segment of sawtooth). For continuous analog input frequencies above Nyquist, the sampled frequency is found by “reflecting off” the aliased frequency lines (heavy dashed segments of sawtooth) in Figure 1B. The instantaneous amplitudes of the illegal signals are added to the amplitude of the frequency to which it is aliased. The aliasing occurs through a folding about multiples of the Nyquist frequency. Immediately

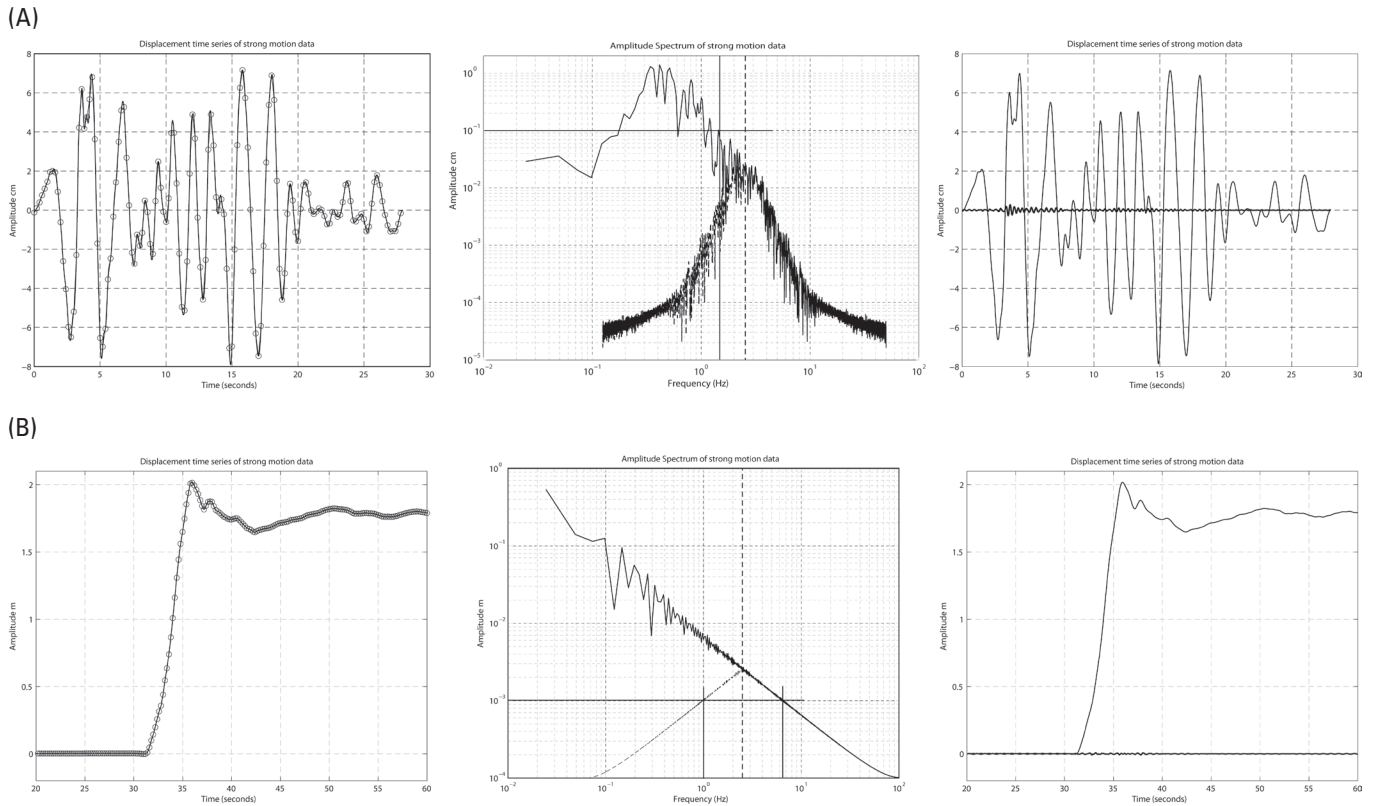


▲ Figure 2. A) Strong-motion east-west displacement time series, integrated twice from acceleration, sampled at 100 Hz from the 1995 **M** 6 Dinar, Turkey, earthquake (Durukal *et al.* 1998) at 3-km epicentral distance. Solid trace in left panel is displacement, with ~2 second period, and ~15 cm peak-to-peak displacement. Black circles and dashed line show a sampling at 1 Hz. Center panel shows amplitude spectrum. The heavy, dashed vertical line identifies the Nyquist frequency for 1-Hz sampling, $f_N = 0.5$ Hz. The leftward sloping dashed reflection of the part of the spectrum above Nyquist shows how the illegal frequency components in the input fold to alias into the legal frequencies. The horizontal line at 1 mm shows the level of GPS resolution, *i.e.*, signal above this level is recorded. The two vertical black lines show the frequencies where the signal and aliased folding reach the level of GPS resolution, 1 mm. The panel on the right shows time series constructed from the legal frequency components (thin, solid trace, low-pass filter with corner at f_N) and illegal, aliased components (heavy, solid trace, high-pass filter with corner at f_N) time series. We will call the heavy solid trace the aliasing signal. B) Strong-motion east-west displacement time series sampled at 200 Hz and integrated twice from acceleration from the 1999 **M** 7.4 Izmit, Turkey, earthquake (Durukal 2002) at a distance of 3.2 km from the surface rupture. Panels follow presentation in Figure 2A. Thin solid trace in left panel shows a steplike, permanent, coseismic displacement of almost two meters.

above Nyquist, input signals are aliased to frequencies just below Nyquist. As the input frequency increases above Nyquist toward the sampling frequency (twice Nyquist), the apparent sampled frequency decreases until, at the sampling frequency, it is aliased to DC. This folding repeats as the frequency continues to increase (Figure 1B). Note there is a simple, fixed relationship between any arbitrary frequency above Nyquist and the frequency between DC and Nyquist into which it is aliased. As the sampling cannot “see” what goes on between samples, if one wants to study the temporal properties or behavior of the analog signal, the analog signal must be restricted such that the continuous behavior between samples can be completely determined, or reconstructed, using only the sampled data. The sampling theorem restricts the input signal based on its frequency-domain representation and requires at least two samples per cycle in the time domain for proper determination of a Fourier component.

BACKGROUND

In general, once a continuous analog signal is sampled, it is impossible to establish whether or not it is aliased. Aliasing must be prevented; it cannot be corrected after sampling. There is only one way to accomplish full-bandwidth, non-aliased recording, and that is to sample fast enough such that there is no measurable energy in the analog input signal at frequencies higher than Nyquist before sampling. This implies one needs an *a priori* knowledge of the signal spectrum to determine the minimum sampling rate. The biggest problem with sampling fast enough is that it may require sampling rates that are prohibitive in terms of transmitting, processing, and archiving the data. The biggest hurdle today is typically the cost of robustly transmitting the data, especially in real time, which, unlike the costs of processing and archiving, is not falling rapidly.



▲ **Figure 3.** A) Same data shown in Figure 2A but analyzed for 5-Hz sampling. Panels follow presentation in Figure 2A modified for 5-Hz sampling. Note that the spectrum is below the GPS resolution of 1 mm before it reaches Nyquist, and the folded portion of the spectrum is always below the resolution, so there is no frequency limit associated with the intersection of the central, heavy, dashed vertical line with the resolution level. The central, heavy, dashed vertical line identifies the 5-Hz sampling Nyquist frequency, $f_N = 2.5$ Hz. B) Same data as in Figure 2B, processed as in 3A. Panels follow presentation in Figure 2A. See text for how to determine the bandwidth of useful legal sampling.

As HRGPS is flat to displacement at seismic frequencies, the key to determining the sampling rate is the resolution of the HRGPS position estimates. Phase-locked-loops, used to track either the phase or code of the GPS signal, can determine phase to $\sim 1\%$ of the wavelength (Hoffman-Wellenhof *et al.* 2001). Phase measurements based on the 19-cm L1 wavelength, the shortest wavelength in the GPS system, provide a resolution of ~ 1.9 mm. Genrich and Bock (2006) report single-epoch horizontal precisions on short baselines that vary with sampling frequency from 1 mm at 1 Hz to 3 mm at 50 Hz. We will use 1 mm as the horizontal resolution, with vertical resolution about a factor of five worse, for the purposes of this discussion. This may be optimistic with today's data, but resolution is improving (Genrich and Bock 2006), and 1 mm is of the correct order of magnitude.

If sampling fast enough is not possible, one has to somehow limit the input signal before sampling to the maximum frequency allowed for alias-free recording (half the sampling rate). The traditional solution is to low-pass filter the signal before sampling such that there is no energy above the Nyquist limit of the sampling frequency. This filtering is called anti-alias filtering. The recorded signal is no longer full bandwidth, and its values will differ from the time series composed of simultaneously determined "true" instantaneous measurements of

the unfiltered analog signal. In the case of HRGPS, anti-alias filtering could be done either mechanically or electronically. To anti-alias filter mechanically, one has to prevent antenna displacements at frequencies higher than Nyquist. This would require a mechanical filtering by the GPS antenna mount, which, while theoretically possible, is impractical and could cause significant problems in long-term monument stability when studying the longer-period geophysical signals measured with GPS. To do it electronically, one could low-pass filter the analog beat phase signal produced in the receiver before sampling, as suggested by Genrich and Bock (2006) for the purpose of improving HRGPS resolution. Because estimating the position from the phase is a linear system, low-pass filtering the phase time series before processing should be equivalent to applying the same filter to the displacement time series after processing. This solution would most likely require redesign of current receiver firmware and/or hardware.

The modern method to accomplish valid digital recording at the desired final sample rate is to oversample (sample the signal much, much more rapidly than needed to ensure valid sampling), digitally low-pass filter the oversampled time series, and finally decimate the oversampled time series to the final, lower sampling rate. This method may include an analog anti-alias filter before the initial sampling, if needed. Advantages of the

oversample-filter-decimate (OFD) method is that one can produce any desired final sampling rate at or below the Nyquist of the initial sampling, the digital anti-alias filter's response can be easily tailored for the final application, and one does not need physical anti-alias filters for each final sampling rate. Another advantage is that it is relatively easy and inexpensive to implement with modern microprocessor technology and oftentimes provides better performance than an analog implementation. Seismologists face the same sampling rate problems for similar reasons. They have the advantage, however, that anti-alias filtering of analog seismometer signals is simple, straightforward, and—in modern broadband instruments—implemented by the manufacturers using the OFD method. Whatever method is used to produce a valid HRGPS time series, comparisons of it to seismic displacements recorded simultaneously should be made with seismic data that has also been properly processed to produce a non-aliased 1-Hz time series.

A number of receivers offer smoothing of either, or both, phase and code as a user-selected option. The specifications of this smoothing, which is some sort of a low-pass filter, and whether it occurs before or after sampling, are typically not published. If this filtering occurs before sampling it could be used to apply the anti-alias filtering. If it is applied after an oversampling, it could be part of an OFD method. The OFD method could also be implemented by streaming oversampled phase data from the receiver to a local computer, which would do the digital filtering, decimation, and recording. This additional processing would only be needed for the stations closest to the major faults, where recording of the motions is potentially aliased, although one does not know before the earthquake which stations will be affected. Generally, at stations farther than several tens of kilometers from the fault, attenuation of the seismic signal by the earth will naturally apply an anti-alias low-pass filter and aliasing will not be a problem, even at 1 Hz.

If one can transmit oversampled HRGPS phase data to the processing center, the digital filtering and decimation can be performed on the displacement time series estimated from the phase data. This would potentially provide the best results but is the most expensive. Genrich and Bock (2006) show that above 0.5 Hz, the noise in HRGPS position time series is white. A significant improvement in resolution, near the theoretical limit, can be obtained by a simple running average (less than two seconds long), which is a low-pass filter followed by decimation. Genrich and Bock (2006) suggest that an initial 100-Hz HRGPS sampling rate could improve the resolution at a final 1-Hz sampling by almost an order of magnitude to order 0.1 mm. Genrich and Bock (2006) also suggest that the averaging (filtering) be performed in the receiver, which implies filtering the phase. While a running average is the best filter for removing random noise and improving the resolution of the averaged data, it is unfortunately among the worst filters as an anti-alias filter (Smith 1997). The improved resolution would also increase the maximum frequency at which displacements are visible by HRGPS, thereby making the aliasing problem worse. The solution is to develop a filter that, at the final sam-

pling rate, simultaneously prevents aliasing while optimizing the improvement in resolution.

The availability of 1-Hz HRGPS phase data is rapidly increasing and has been used to determine displacement time histories in the epicentral region of earthquakes (*e.g.*, the 2002 Denali earthquake: Larson *et al.* 2003; Bilich *et al.* 2008), provide near-field displacement time series for inversion of fault slip (*e.g.*, 2003 San Simeon earthquake: Ji *et al.* 2004; Wang *et al.* 2007; the Tokachi-Oki (Hokkaido) earthquake: Miyazaki *et al.* 2004), for teleseismic observation of surface waves (Larson *et al.* 2003; Ohta 2006), and to measure surface wave dispersion curves from the great 2004 Sumatra-Andaman earthquake (Davis and Smalley, forthcoming). The latter two applications examine large-amplitude, low-frequency signals faithfully recorded at 1 Hz. This can be demonstrated using spectral analysis of co-located broadband seismograph recordings of the same waves (Bilich *et al.* 2008; Davis and Smalley, in press). Potential problems arise with the first two applications, where ground displacement time history at very small epicentral distances from large and great earthquakes can contain measurable energy above Nyquist (0.5 Hz for 1-Hz sampling), as is demonstrated in Figures 2A and B. It is these situations where HRGPS offers the most promise, as it complements strong-motion acceleration data by estimating displacement time histories directly without the problems of doubly integrating acceleration (Boore *et al.* 2002). GPS also has much higher clipping limits than broadband seismometers and most strong-motion accelerometers. Note that the theoretical clipping limits for GPS come from the GPS receiver's phase-locked-loop's ability to track the phase. The acceleration changes the rate of change of the phase and determines when GPS "clips." The accelerations associated with earthquakes are much smaller than the limits of the typical GPS receiver's electronics, and clipping of the GPS receiver is not considered a problem in HRGPS seismology. Practically, the performance of commercial GPS receivers is limited by the U.S. Department of Commerce rather than the electronics (Coordinating Committee on Multilateral Export Controls [COCOM] limits on velocity and altitude, with some manufacturers additionally specifying arbitrary acceleration and jerk limits). Acceleration limits, when they exist or are specified, are typically above 4 g, which is greater than the magnitudes of the accelerations observed from earthquakes.

Current Plate Boundary Observatory (PBO) GPS receivers can record as fast as 10 Hz, while rates up to 50 Hz or higher are currently available in other commercial equipment and have been used for meteorological applications of GPS (GPS MET) and ionospheric scintillation studies (Wickert *et al.* 2001; Beyerle *et al.* 2001), seismic engineering (Bock *et al.* 2006), and geodesy (Genrich and Bock 2006). PBO currently continuously records and archives data sampled at 30-sec epochs and continuously records 5-Hz data in a ring buffer in the receiver. Due to bandwidth and cost considerations, the 5-Hz data is downloaded and archived only upon triggering by a predefined set of earthquakes or other signals or upon request. The phase smoothing and multipath reduction options of the receiver are

disabled. As we will see, for the most important potential events in the PBO footprint, such as an **M** 7–8 on the San Andreas fault or a megathrust in Cascadia, a sampling rate of 5 Hz for the displacement time series will most likely not be fast enough, yet a sampling rate for the displacement time series as fast as 50 Hz will also not be required, at least as far as aliasing is concerned. This discussion complements the work of Genrich and Bock (2006), Choi and Larson (2006), and Clinton *et al.* (2007), all of which concentrate on the quality and application of HRGPS data and also address the important issues of temporal fidelity and aliasing of HRGPS data.

DISCUSSION

Several large earthquakes have been well recorded by strong-motion accelerometers in the very near-field, and these data can provide the *a priori* knowledge of the spectrum associated with dynamic coseismic motions needed to determine HRGPS sampling rates. We will now present the analysis of strong-motion data recorded within a few kilometers of the fault rupture plane for two earthquakes and examine the implications for HRGPS, for which raw 1-Hz sampling is generally accepted to be sufficient. In these two examples, we will first doubly integrate the acceleration, which has been sampled fast enough to avoid aliasing, to displacement. We will then show how analysis of the displacement signal is affected, in both the time and frequency domains, by sampling at various frequencies. Examining the input in the time domain after high- and low-pass filtering with Nyquist cutoff shows the valid and illegal signals that are sampled, and then summed, at the given sampling rate. Analysis in the frequency domain shows how the signal from above Nyquist folds into the legal frequency band, which ranges from DC to Nyquist, where it combines with the legal spectra. The net effect on amplitude in the frequency domain is not a simple summation due to the phase, which is why we cannot use knowledge of the amplitude spectrum to correct for aliasing. Assuming the displacement time series represents the position of the ground as a function of time, whether or not a sampling is aliased is a function of the sampling rate, the signal spectrum, and the resolution of the measurement technology. As GPS and accelerometer resolutions are not equal, they will require different sampling rates for valid, non-aliased recording. Figures 2 and 3 show displacement time series, doubly integrated from acceleration, and amplitude spectra for the 1995 **M** 6 Dinar, Turkey, earthquake (Durukal *et al.* 1998) and the 1999 **M** 7.4 Izmit or Kocaeli, Turkey, earthquake (Durukal 2002). These earthquakes were chosen because of the availability of high quality strong-motion data from very small epicentral distances. The Izmit earthquake is also similar, in both size and mechanism, to a probable event on the San Andreas fault system.

The left panel of Figure 2A for the Dinar earthquake shows a 1-Hz sampling of the continuous-looking displacement sampled at 100 Hz. For non-aliased recording, Nyquist has to be above all frequency components having sufficient amplitude such that they can be recorded by HRGPS. In the central panel of Figure 2A we see that for 1-Hz sampling, Nyquist is very near

the maximum of the spectrum where the spectral amplitude is of order 1 cm. The results of a high-pass filtering, using the Nyquist frequency for 1-Hz sampling as the cutoff frequency, is shown by the heavy trace in the rightmost panel. This trace has a significant signal with >5 cm peak-to-peak amplitude. This means the signal from the spectral components immediately above Nyquist is large enough to be recorded by HRGPS. The signal amplitude from the aliased (illegal) frequencies is ~30% of the total input signal amplitude, and ~40% of the amplitude of the non-aliased (legal or valid) portion of the input signal, which is shown by the thin trace after low-pass filtering with a cutoff at Nyquist. The time series sampled at 1 Hz in the left panel is aliased and should not be used for spectral analysis or fault slip inversion. For this normal faulting event, the accelerometer was close to the hanging wall block but outside the region of permanent coseismic displacement. The average acceleration and velocity over the duration of the event are zero and the displacement time series records the passage of near-source seismic waves and returns to zero after their passage.

A similar analysis for the Izmit earthquake is shown in Figure 2B. For this event, the accelerometer was 3.2 km from the vertical rupture plane of the east-west-striking strike-slip fault and in the region of permanent coseismic displacement. While the acceleration and velocity return to zero after the event, their averages over the duration of the event are nonzero, which results in a non-zero displacement. The displacement time series represents the development of the permanent elastic deformation and the transient, very near-field seismic waves. The amplitude spectrum shows the amplitude in the vicinity of Nyquist is of the order of centimeters. Note that the amplitude spectrum is that expected for a step function, which the displacement approximates. Results of high-pass filtering with a Nyquist cutoff show a significant signal, ~16 cm peak-to-peak amplitude, from the frequency components beyond Nyquist. The time series after sampling at 1 Hz is aliased. In this case, the illegal signal is about 10% of the valid signal amplitude of ~2 m. The contamination from the aliasing signal varies from 50% at Nyquist to 10% at 0.2 Hz (five-second period), and spectral analysis based on this recording is not recommended. Note that compared to the Dinar earthquake, while the absolute amplitude of the aliased contribution here is larger, the percent amplitude of the aliased contribution is much smaller.

In Figure 3 the same data shown in Figure 2 are examined using a 5-Hz sample rate. For the Dinar earthquake (Figure 3A), the amplitude in the vicinity of Nyquist is down to several tenths of a millimeter. In the right panel, the heavy trace (aliasing signal) has maximum amplitude during a short period at the beginning of the record of ~3 mm peak-to-peak (5% of the max valid amplitude) in the high-pass filtered signal beyond Nyquist. This is near the 1-mm resolution we are using for HRGPS. The amplitude spectra shows the time series sampled at 5 Hz is valid and could be safely used for spectral analysis or fault slip inversion, especially if the highest frequency components that produce the aliasing signal, as will be discussed later, were not used.

The spectral analysis of the 5-Hz sampling for the Izmit earthquake shows it is also aliased. In this case we can sal-

vage the situation by appropriate processing in the frequency domain. The maximum frequency with valid, non-aliased recording is determined by finding the frequency at which the aliased signal is too small to be recorded by HRGPS, 1 mm. This is shown in the center panels of Figure 3B, where the illegal Fourier components are folded into their aliased counterparts and the folded spectrum (leftward sloping dashed reflection of the spectrum above Nyquist) falls to 1 mm at 1 Hz. The frequency components up to 1 Hz are uncontaminated by aliasing, while those above 1 Hz are contaminated by the contribution of energy from the aliased frequencies. The aliasing signal, even though small in terms of percentage, is large enough to be well recorded by HRGPS, and the high-frequency components in analyses, such as an inversion for fault slip, would be affected. The contamination is small at 1 Hz and grows as Nyquist is approached. By limiting analysis in the frequency domain to frequencies below 1 Hz, or by using this limit as the corner for a low-pass filter when transforming back to the time domain, we can perform valid analysis of these data in the time or frequency domains (this is a modification of the OFD idea). This technique only works when the frequency limit of the aliased data is close to Nyquist and leaves sufficient bandwidth below the limit to make useful measurements. This is not the case for the 1-Hz data shown in Figures 2A and 2B, where the aliased data at 1-mm amplitude wrap significantly back toward DC. In these cases, the aliased frequency value at 1-mm amplitude is ~ 0.2 Hz (five-second period) and 0.04 Hz (25-second period), respectively, leaving only a few of the lowest frequencies uncontaminated by aliased data. This technique clearly fails when the aliased sampled frequency limit wraps back to, or past, DC, and all the data in the frequency domain would be affected by aliasing. The biggest problem with this method is that without having a detailed *a priori* knowledge of the spectrum, one cannot identify the frequency limit where aliased energy becomes important in the frequency domain. “Pushing” the data in these situations will ensure that aliased energy is included in the frequency and time-domain representations of the signal.

Huang and Wang (2002) examined displacement records integrated from acceleration from the 1999 M_S 7.6 Chi-Chi earthquake. This thrust event produced 400–700 cm of coseismic offset, 1.5–2.2 cm/sec peak velocity, and peak acceleration of $\sim 0.4g$. A spectral amplitude of 1 mm was reported out to 5 Hz for a site in the hanging wall block that was approximately 1 km above the dipping fault plane (Huang and Wang 2002). In a similar analysis (not shown) of the displacement time series recorded by an accelerometer located on the hanging wall of the 1994 M_W 6.7 Northridge, California, earthquake, significant energy is also found above Nyquist for 1-Hz sampling. The Northridge earthquake produced a maximum of ~ 42 cm vertical, and ~ 2.2 m horizontal, static coseismic thrust displacements (Hudnut *et al.* 1996). This situation is similar to that of the Izmit earthquake in that 5-Hz sampling may produce useful data. Without an *a priori* detailed knowledge of the spectrum one is not sure if the upper frequency limit of alias-free recording is at Nyquist (2.5 Hz) or some lower frequency.

CONCLUSIONS

Realizing the potential contribution of HRGPS displacement time series to quantify the dynamic deformations in the very near-field of large and great earthquakes requires assurance that the data recorded by the HRGPS stations are a valid representation of the ground displacement temporal history and are not contaminated by aliasing. We have shown that 1-Hz HRGPS recordings of dynamic displacements at very small (several kilometer) epicentral distances from earthquakes as small as M 6 are aliased and should not be used for spectral analyses or inversions for source parameters. For M 7 and larger events, sampling at 5 Hz may also be aliased, but in some cases not so badly that it cannot be salvaged by appropriately limiting the uppermost frequency used in the analysis. These aliasing problems are limited only to the stations that are extremely close to the fault, although the distance to which aliasing has to be considered will increase with increasing magnitude. Some sort of anti-alias filtering (receiver processing, local OFD, etc.) is needed for a final 1-Hz sampling rate within ~ 10 km of the major faults to ensure they record usable, valid data. The cases examined suggest that for stations very close to the fault, sampling at 10 Hz, which has a 5-Hz Nyquist, would produce relatively alias-free recordings for steplike permanent displacements of up to at least three meters, such as those that would be expected from a 1906-sized event on the San Andreas. In the very near-field the displacement time series for such an event would consist of a step-function-like coseismic displacement associated with elastic rebound plus any recovery from dynamic overshoot and the near-source seismic wavefield. In the example from Izmit, the coseismic offset term dominated the displacement time series. For megathrust events in Cascadia, the coseismic offset on the fault plane may approach 10–20 m. For a pure elastic rebound coseismic step function, the amplitudes in the frequency domain will scale by the same factor as the size of the offset. The GPS stations in this case may be far enough away from the fault plane, at least 10–20 km vertically, that the earth will low-pass-filter the data. These sites may record non-aliased data at sampling frequencies as low as 1 Hz, but due to attenuation they may not require sampling as high as 10 Hz, and 5-Hz sampling would probably be sufficient. In this case, the high-frequency energy, while significant, is dwarfed by the much larger low-frequency signal. The most problematic events may be the M 6–7.5 events, such as Dinar and Northridge, where, for 1-Hz sampling at small distances, the seismic energy peaks near Nyquist. Sampling at frequencies higher than necessary would allow proper anti-alias filtering and improved resolution for the final processed time series. ☒

ACKNOWLEDGMENTS

Strong-motion acceleration data from the Izmit earthquake were obtained from the European Strong-Motion Database (Ambraseys *et al.* 2002), and the displacement data for the Dinar earthquake were graciously provided by E. Durukal and M. Erdik via e-mail. Strong-motion displacement data from the

Northridge earthquake were obtained from the Consortium for Strong-Motion Observation Systems (COSMOS) Virtual Data Center (Archuleta *et al.* 2006). The manuscript was improved through reviews by M. Hamburger, K. Larson, an anonymous reviewer, and Eastern Section editor M. Chapman. This work was supported in part by the Mid-America Earthquake Center (MAEC), an Earthquake Engineering Research Center of the National Science Foundation, under award number EEC-9701785.

REFERENCES

- Ambraseys, N., P. Smit, R. Sigbjornsson, P. Suhadolc, and B. Margaris (2002). Internet-Site for European Strong-Motion Data, European Commission, Research-Directorate General, Environment and Climate Programme, <http://www.isesd.cv.ic.ac.uk/ESD/frameset.htm>.
- Archuleta, R. J., J. Steidl, and M. Squibb (2006). The COSMOS Virtual Data Center: A web portal for strong motion data dissemination. *Seismological Research Letters* **77** (6), 651–658.
- Beyerle, G., J. Wickert, R. Galas, K. Hocke, R. König, C. Marquardt, A. G. Pevely, C. Reigber, and T. Schmidt (2001). GPS occultation measurements with GPS/MET and CHAMP. *Taikiken Shinpojiumu* **15**, 44–77.
- Bilich, A., J. F. Cassidy, and K. M. Larson (2008). GPS Seismology: Application to the 2002 M_w 7.9 Denali fault earthquake. *Bulletin of the Seismological Society of America* **98** (2), 593–606; doi: 10.1785/0120070096.
- Bock, Y., L. Prawirodirdjo, and T. I. Melbourne (2004). Detection of arbitrarily large dynamic ground motions with a dense high-rate GPS network. *Geophysical Research Letters* **31**, L06604; doi:10.1029/2003GL019150.
- Bock, Y., M. Panagiotou, F. Yang, J. Restrepo, and J. Conte (2006). Shake table tests of a full scale reinforced concrete wall building: Real time 50 Hz GPS displacement measurements (abstract). *Seismological Research Letters* **77** (2), 216.
- Boore, D. M., C. D. Stephens, and W. B. Joyner (2002). Comments on baseline correction of digital strong-motion data: Examples from the 1999 Hector Mine, California, earthquake. *Bulletin of the Seismological Society of America* **92** (4), 1,543–1,560.
- Choi, K., and K. Larson (2006). Assessment of GPS errors from 0.01 to 10 Hz. *Eos, Transactions, American Geophysical Union* **87** (52), Fall meeting supplement, abstract G33A-0036.
- Clinton, J. F., K. Larson, and A. Bilich (2007). High-rate GPS Data—when are they useful? *Eos, Transactions, American Geophysical Union* **88** (52), Fall meeting supplement, abstract G13B-1235.
- Davis, J. P., and R. Smalley Jr. (forthcoming). Love wave dispersion in central North America determined using high rate GPS absolute displacement seismograms. *Journal of Geophysical Research*.
- Durukal, E., M. Erdik, J. Avcı, Ö. Yüzügüllü, Y. Alpaya, B. Avar, C. Zülfiyar, T. Biro, and A. Mert (1998). Analysis of the strong motion data of the 1995 Dinar, Turkey earthquake. *Soil Dynamics and Earthquake Engineering* **17**, 557–578.
- Durukal, E. (2002). Critical evaluation of strong motion in Kocaeli and Düzce (Turkey) earthquakes. *Soil Dynamics and Earthquake Engineering* **22**, 589–609.
- Genrich, J. F., and Y. Bock (2006). Instantaneous geodetic positioning with 10–50 Hz GPS measurements: Noise characteristics and implications for monitoring networks. *Journal of Geophysical Research* **111**, B03403; doi:10.1029/2005JB003617.
- Hoffman-Wellenhof, H. Lichtenegger, and J. Collins (2001). *Global Positioning System: Theory and Practice*. Fifth rev. ed. New York: Springer-Verlag, 370 pps.
- Huang, M.-W., and J.-H. Wang (2002). Scaling of displacement spectra of near-fault seismograms of the 1999 Chi-Chi, Taiwan, earthquake. *Geophysical Research Letters* **29** (10), 1,442; doi: 10.1029/2001GL014021.
- Hudnut, K. W., Z. Shen, M. Murray, S. McClusky, R. King, T. Herring, B. Hager, Y. Feng, P. Fang, A. Donnellan, and Y. Bock (1996). Co-seismic displacements of the 1994 Northridge, California, earthquake. *Bulletin of the Seismological Society of America* **86** (1B), S19–S36.
- Ji, C., K. M. Larson, Y. Tan, K. W. Hudnut, and K. Choi (2004). Slip history of the 2003 San Simeon earthquake constrained by combining 1-Hz GPS, strong motion, and teleseismic data. *Geophysical Research Letters* **31**, L17608; doi:10.1029/2004GL020448.
- Larson, K., P. Bodin, and J. Gombert (2003). Using 1-Hz GPS data to measure deformations caused by the Denali fault earthquake. *Science* **300**, 1,421–1,424.
- Miyazaki, S., K. M. Larson, K. Choi, K. Hikima, K. Koketsu, P. Bodin, J. Haase, G. Emore, and A. Yamagiwa (2004). Modeling the rupture process of the 2003 September 25 Tokachi-Oki (Hokkaido) earthquake using 1-Hz GPS data. *Geophysical Research Letters* **31**, L21603; doi:10.1029/2004GL021457.
- Nyquist, H. (1928). Certain topics in telegraph transmission theory. *Transactions of the American Institute of Electrical Engineers* **47** (April 1928), 617–644; reprinted as a classic paper in *Proceedings of the IEEE* **90** (2), 280–305.
- Ohta, Y., I. Meilano, T. Sagiya, F. Kimate, and K. Hirahara (2006). Large surface wave of the 2004 Sumatra-Andaman earthquake captured by the very long baseline kinematic analysis of 1-Hz GPS data. *Earth Planets Space* **58**, 153–157.
- Shannon, C. E. (1949). Communication in the presence of noise. *Proceedings of the Institute of Radio Engineers* **37** (1), Jan. 1949, 10–21; reprinted as a classic paper in *Proceedings of the IEEE* **86** (2), 447–457.
- Smith, S.W. (1997). *The Scientist and Engineer's Guide to Digital Signal Processing*. San Diego: California Technical Publishing.
- Unser, M. (2000). Sampling—50 years after Shannon. *Proceedings of the IEEE* **88** (4), 569–587.
- Wang, G. Q., D. M. Boore, G. Tang, and X. Zhou (2007). Comparisons of ground motions from collocated and closely spaced one-sample-per-second global positioning system and accelerograph recordings of the 2003 M 6.5 San Simeon, California, earthquake in the Parkfield region. *Bulletin of the Seismological Society of America* **97** (1B), 76–90; doi: 10.1785/0120060053.
- Wickert, J., C. Reigber, G. Beyerle, R. König, C. Marquardt, T. Schmidt, L. Grunwaldt, R. Galas, T. K. Meehan, W. G. Melbourne, and K. Hocke (2001). Atmosphere sounding by GPS radio occultation: First results from CHAMP. *Geophysical Research Letters* **28**, 3,263–3,266.

Center for Earthquake Research and Information
University of Memphis
Memphis, Tennessee 38152 U.S.A.
rsmalley@mempis.edu